UDC 621.372

ANALYSIS OF MICROSTRIP STRUCTURES BY NUMERICAL CONFORMAL TRANSFORMATIONS TECHNIQUE

Alexander N. Sychev, Mikhail A. Chekalin, Vasily A. Shestakov

Tomsk State University of Control Systems and Radioelectronics (TUSUR), Tomsk, Russia

Computer aided microstrip structures modeling has been performed by conformal mapping technique. A new approach to reduce the connectivity order of the original cross-section geometry of the structure is proposed. The multiply connected domain is reduced to simply connected ones by implementation of magnetic slits concept. The microstrip structures analysis is carried out by numerical conformal transformations technique realized in Schwarz–Christoffel toolbox for MATLAB. This technique is applied to the quasi-static analysis of coupled microstrip lines taking into account the conductor thickness. Described approach ensures high numerical efficiency and can be used for accurate analysis of complex microstrip structures.

Introduction

Coupled microstrip lines and other microstrip structures are widely used in high-speed digital and analog microwave integrated circuits [1—3]. Their main features are the complexity of the cross-section geometry and the inhomogeneity of the dielectric filling. Successful designing of the modern integrated circuits is impossible without the implementation of accurate and computationally effective methods for their characterization [4].

There is no single universal approach satisfying all the criteria to the analysis of stripline structures. Using three-dimensional and two-dimensional electromagnetic methods ensured the sufficient accuracy is associated with a large amount of computer time. Hence, methods of boundary elements, finite differences, integral equations based on quasi-static approach can be considered as capable for successful complicated microstrip structures analyzing. Among them, the conformal mapping technique (CMT) with high-speed computer implementation seems to be a quite attractive method for solving this needful problem.

The conformal mapping technique is widely used to analyze the various stripline structures due to its distinctive features [4—13]. Highest computational efficiency of algorithms and programs which do not require significant computing resources allows creating the fast CAD as well as easily inserting the procedures of the multivariate analysis, optimization and synthesis of complex microstrip structures into the programs. The conformal mapping technique is well combined with other analytical and numerical methods of electromagnetic modeling.

Using the Schwarz–Christoffel integral (SCI) for simply connected polygonal regions allows obtaining exact analytical solutions that are reliable benchmarks for the numerical testing of other methods. High clarity of the conformal mapping approach ensures the possibility of visualizing the field by building a network of equipotential and force lines.

The Schwarz–Christoffel mapping technique is continued to be an area of active research. Specialized numerical procedures and computer programs are created for practical implementation of SCI. The Schwarz–Christoffel toolbox for MATLAB [14] as a public-domain package was created on the base of Trefethen's FORTRAN package. First version of this open source software was developed by Driscoll in 1994, and the last version appeared in 2007 [15, 16]. The Schwarz–Christoffel toolbox is used in present work.

Analysis procedure

Due to the complexity of cross-section and inhomogeneity of the dielectric filling of the microstrip structures, their simulation are performed with the use of the decomposition operations and taking into account: the symmetry of the structure; the type of modal excitation and the periodicity properties for the multiconductor structures; the type of the interface between dielectrics in two- and multilayered structures.

Fig. 1 schematically presents the microstrip line analysis procedure consisting of the following steps:

1. *Reduction through symmetry.* Cross-section of the microstrip structure is subjected to preliminary decomposition. A symmetry plane (if it exists in principle) is introduced. Depending on the excitation mode, the symmetry plane can be displayed by either magnetic or electric wall.

2. *Reducing the connectivity of the cross-section region by magnetic slits.* The obtained partial cross-sectional regions t are multiply connected. To reduce

the order of connectivity to the simply connected *w*, symmetrical slits along magnetic walls are introduced between external border and internal electrodes. These heuristically imposed magnetic slits should not disturb the structure of the field for a given excitation mode (which is possible if the slit is laid along the force line). This very important step greatly determines the accuracy of the technique schematically presented in Fig. 1.

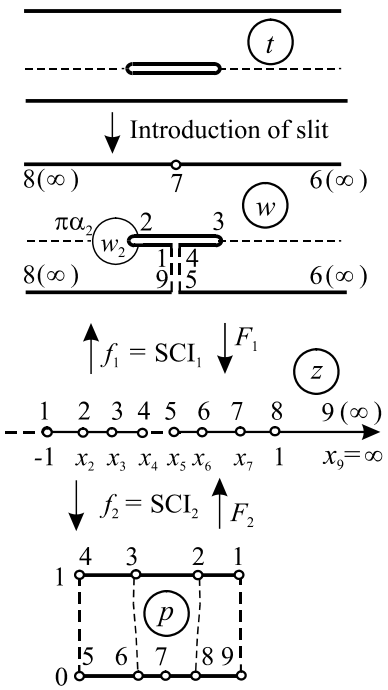

Fig. 1. Original cross-section geometry of the strip structure and its transformation by cutting and by mapping into the upper half-plane, and then into the target rectangular region (parallel-plate capacitor).

3. *First Schwarz–Christoffel mapping into the canonical domain.* Taking into account the conductor thickness, each of the obtained simply connected polygonal region *w* is conformally mapped into the canonical domain *z* which is either the upper half-plane or the interior of the unit disk. At the same time, both forward $z = F_1(w) = f_1^{-1}(w) = \mathrm{SCI}_1^{-1}(w)$ and inverse $w = F_1^{-1}(z) = f_1(z) = \mathrm{SCI}_1(z)$ mappings should be created.

4. *Second Schwarz–Christoffel mapping into the target rectangular domain as a parallel-plate capacitor.* The canonical domain *z* obtained in the previous stage is mapped into the final target rectangular domain *p* in the form of the parallel-plate capacitor. At the same time, both forward $p = f_2(z) = \mathrm{SCI}_2(z) = F_2^{-1}(z)$ and inverse $z = f_2^{-1}(p) = \mathrm{SCI}_2^{-1}(p) = F_2(p)$ mappings should be created.

The composite forward mapping from the original polygon *w* into target rectangle *p* can be written as

$$p = \mathrm{SCI}_2[\mathrm{SCI}_1^{-1}(w)]. \quad (1)$$

This forward mapping relation can be used to determine the dielectric-dielectric interface curve in the target rectangle.

The composite inverse mapping from the target rectangle *p* into original polygonal region *w* can be presented by following relation:

$$w = \mathrm{SCI}_1[\mathrm{SCI}_2^{-1}(p)]. \quad (2)$$

This inverse mapping expression will be employed to determinate the electric field distribution in the original microstrip structure.

Using the obtained formulas we can find the capacitance per unit length of the structure (parallel-plate capacitor) filled with air dielectric $C(1)$. It is the ratio of the width of electrodes to the distance between them.

5. *Accounting the inhomogeneity*. The next step is intended to find the curve between dielectrics in the parallel-plate capacitor *p*. In particular, it is the air-dielectric boundary, corresponding to the surface of the substrate in the initial microstrip structure *t*. Using relation (1) and Zehentner's technique [9] which allow accounting the inhomogeneity, we can find the capacitance per unit length of the parallel-plate capacitor with real dielectric filling *C*.

6. *Calculating other quasi-static parameters*. For even/odd excitations of coupled lines we have already defined the even/odd mode capacitances per unit length with the air dielectric $C(1)_{(e,o)}$ and with real dielectric filling $C_{(e,o)}$. That allows calculating even/odd mode effective permittivities $\varepsilon_{eff\,(e,o)}$ and characteristic impedances $Z_{0(e,o)}$, as well as *L* and *C* matrices.

Schwarz–Christoffel mapping

The Schwarz–Christoffel conformal mapping technique maps the upper half of the complex plane into a simply connected polygonal region [1], [15]. A simply connected region can be defined as the interior of a planar closed line which does not contain any holes. A new formula for the mapping of the multiply connected regions was recently derived by Crowdy [17]. This formula allows obtaining correct results [18] but it is complicated and inconvenient for practical computations.

The basic SCI is a formula for the conformal map *f* from the complex upper half-plane (the canonical domain) to the interior of a polygon (the physical domain) [16]. The polygon may have cracks or vertices at infinity as indicated in Fig. 1. Its vertices are denoted by $w_1, w_2, \ldots, w_n$ and the numbers $\alpha_1\pi, \alpha_2\pi, \ldots, \alpha_n\pi$ designate the interior angles at vertices. The real preimages of the vertices, or pre-vertices, denoted by $x_1, x_2, \ldots, x_n$ are satisfied the condition

$$x_1 < x_2 < \ldots < x_n = \infty .$$

If vertex w_k is finite, then $0<\alpha_k \le 2$. If w_k is infinite, $-2 \le \alpha_k \le 0$. Supposing the necessary constraint

$$\sum_{k=1}^{n} \alpha_k = n - 2 ,$$

we obtain the SCI formula for the map f

$$w = f(z) = f(z_0) + A \int_{z_0}^{z} \prod_{k=1}^{n-1} (z - x_k)^{\alpha_k - 1} dz =$$

$$= w_0 + A \int_{z_0}^{z} (z - x_1)^{\alpha_1 - 1} (z - x_2)^{\alpha_2 - 1} \ldots (z - x_{n-1})^{\alpha_{n-1} - 1} dz \quad (3)$$

where A and z_0 are complex constants. In most cases, it can be assumed that $z_0 = 0$ and $w_0 = f(z_0)$.

The main practical difficulty with this formula is that the pre-vertices x_k cannot be computed analytically except in special cases. Three pre-vertices including the already fixed x_n can be chosen arbitrarily. The remaining $n-3$ pre-vertices are then determined uniquely. They can be obtained by solving a system of nonlinear equations. This technique is known as the Schwarz–Christoffel parameter problem. Its solution is the first step in any Schwarz–Christoffel map. When solving the parameter problem, the multiplicative constant A can be found, and f and its inverse can be computed numerically.

Composing (3) with standard conformal maps leads to variations of the Schwarz–Christoffel formula for mapping from other fundamental domains. The simplest modification of this formula can be obtained by using the unit disk $|z|<1$ as its domain. The pre-vertices then lie in counterclockwise order on the unit circle $|z_k|=1$, and the resulting formula is identical to known one except that there are n rather than n–1 terms in the product of the integrand [13, 15].

Example of modeling

To test the proposed technique of analysis, we consider coupled microstrip lines (CMSL), shown in Fig. 2.

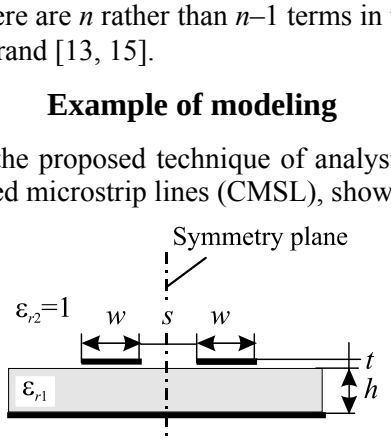

Fig. 2. Geometry of coupled microstrip lines with a designation of the vertical symmetry plane and the horizontal plane between dielectrics.

Conformal mappings of the coupled microstrip lines half-structure for even and odd mode excitations are shown in Fig. 3 and in Fig. 4, respectively. They correspond to steps 1–4 of proposed technique. Let us consider the implementation of these steps in detail.

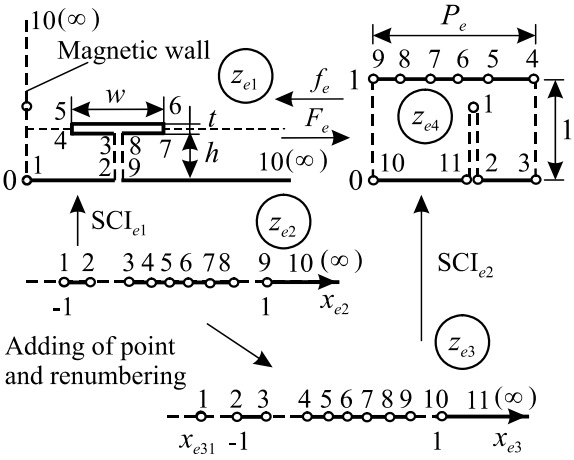

Fig. 3. Conformal mapping of the coupled microstrip lines half-structure for even mode.

When forming the following vector of angles $\alpha_1 = (0.5, 0.5, 0.5, 1.5, 1.5, 1.5, 1.5, 0.5, 0.5, -0.5)$ in original even polygon z_{e1} according to Fig. 3, we get the first SCI

$$z_{e1} = A_e \int_{x_{e21}}^{z_{e2}} \frac{\prod_{k=4}^{7} \sqrt{z_{e2} - x_{e2k}}}{\prod_{k=1}^{3} \sqrt{z_{e2} - x_{e2k}} \cdot \prod_{k=8}^{9} \sqrt{z_{e2} - x_{e2k}}} dz_{e2} , \quad (4)$$

where A_e is a constant to be determined; x_{e2k} are real pre-vertices lying on the real axis x_{e2} of the complex half-plane z_{e2}.

Now, we can find the coordinate of the additional point x_{e31} numerically, for instance, by the bisection method. Then, forming a new real vector x_{e3} consisting of additional point x_{e31} and vector x_{e2} from sequence $x_{e3} = (x_{e31} \ldots x_{e2})$, as well as corresponding renumbering allows obtaining the next half-plane z_{e3} (Fig. 3).

When forming the following vector of angles $\alpha_e = (2, 0.5, 0.5, 0.5, 1, 1, 1, 1, 0.5, 0.5, 0.5)$ in even target polygon z_{e4} according to Fig. 3, we get the second SCI

$$z_{e4} = \int_{x_{e310}}^{z_{e3}} \frac{z_{e2} - x_{e31}}{\prod_{k=2}^{4} \sqrt{z_{e2} - x_{e3k}} \cdot \prod_{k=9}^{10} \sqrt{z_{e2} - x_{e3k}}} dz_{e3} , \quad (5)$$

where x_{e3k} are pre-vertices lying on the real axis x_{e3} of the complex half-plane z_{e3}. Now, we can determine the capacitance per unit length of coupled microstrip lines with air dielectric filling for even mode as follows:

$$C_e(1) = \varepsilon_0 P_e, \quad (6)$$

where $\varepsilon_0 = 8.854$ pF/m is dielectric permittivity of the free space; P_e denotes the width of the rectangle even region z_{e4} with normalized height equaled to unity.

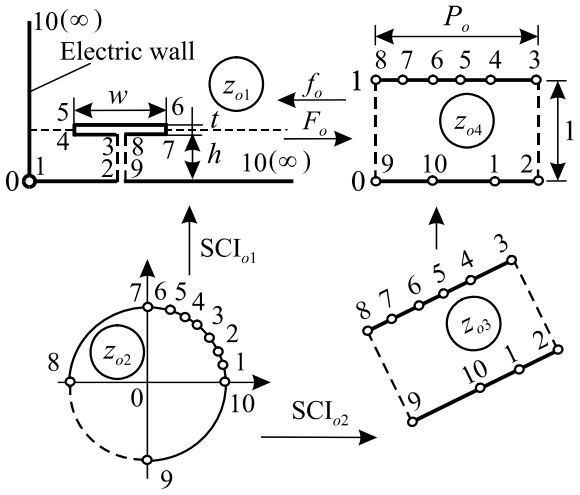

Fig. 4. Conformal mapping of the half-structure of the coupled microstrip lines for odd mode.

Fig. 4 illustrates the process of conformal transformation for odd mode. Taking into account angles in original odd polygon z_{o1} forming the same vector α_1 as in even polygon z_{e1}, we get the first SCI for odd mode

$$z_{o1} = A_o \int_{z_{o210}}^{z_{o2}} \frac{\prod_{k=4}^{7} \sqrt{z_{o2} - z_{o2k}}}{\prod_{k=1}^{3} \sqrt{z_{o2} - z_{o2k}} \cdot \prod_{k=8}^{9} \sqrt{z_{o2} - z_{o2k}}} dz_{o2}, \quad (7)$$

where A_0 is a complex constant; z_{o2k} are pre-vertices lying counterlockwise on the unit disk $|z_{o2}| = 1$. The vector of angles in odd target rectangular region z_{o4} is $\alpha_o = (1, 0.5, 0.5, 1, 1, 1, 1, 0.5, 0.5, 1)$, therefore the second SCI for odd mode can be written as:

$$z_{o3} = \int_{z_{o29}}^{z_{o2}} \frac{dz_{o2}}{\prod_{k=2}^{3} \sqrt{z_{o2} - z_{o2k}} \cdot \prod_{k=8}^{9} \sqrt{z_{o2} - z_{o2k}}}, \quad (8)$$

where z_{o2k} are pre-vertices lying counterlockwise on the unit disk $|z_{o2}| = 1$.

Subsequent normalization z_{o3} leads to rectangular region z_{o4} oriented along axes. Now, the target region z_{o4} can be presented as parallel-plate capacitor having the following capacitance per unit length with air dielectric filling

$$C_o(1) = \varepsilon_0 P_o \quad (9)$$

where P_o is the width of the odd rectangular region z_{o4} with normalized height equaled to unity.

The composite inverse mappings (2) from the target rectangular regions z_{e4} and z_{o4} into original polygonal regions z_{e1} and z_{o1} allow finding the electric field distribution in the analyzed microstrip structure. For this, we generate rectangular grids of the force and the equipotential lines in the target rectangular regions z_{e4} and z_{o4}. Then, using (2), we map those grids into original polygonal regions z_{e1} and z_{o1}, corresponding to the analyzed microstrip structures for even and odd mode excitation. Calculated distributions of the electric field in the coupled microstrip lines half-structure for the even and odd modes are shown in Fig. 5.

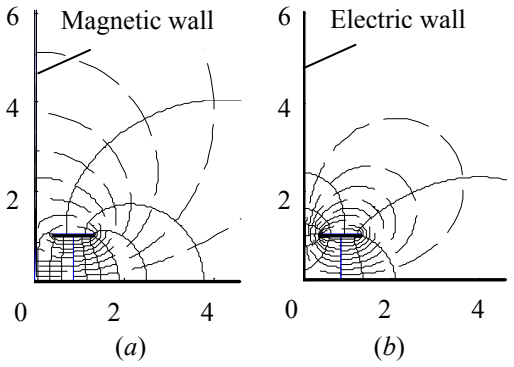

Fig. 5. Calculated distributions of the force (solid curves) and the equipotential (dashed curves) of the electric field in the coupled microstrip lines half-structure for even (*a*) and odd (*b*) modes.

The resulting maps of the electric field (Fig. 5) allow making sure in adequacy of introduced magnetic slits shown in Fig. 3 and Fig. 4.

Conformal mapping of inhomogeneous dielectric boundaries

Taking into account the dielectric inhomogeneity of the microstrip structures has been performed by many authors. Wheeler [10] has proposed an approach to analysis of a single microstrip line based on concept of parallel capacitor and has obtained the relation between the effective filling fraction *q* and the effective dielectric constant ε_{eff}.

Later Wan [11] analyzed the coupled microstrip lines considering the air-dielectric boundary as an elliptical-looking curve. He assumed the boundary to be a quarter of the ellipse and applied the equivalent boundary approximation to get the dielectric filling factor and the mode effective permittivity.

By using the mechanism of the Jacobi functions, Callorotti [12] obtained the solution based on sequential forward and reverse Schwarz–Christoffel transforma-

tions. He separated the dielectric interface function into real and imaginary parts. It allowed the analytical determining the curve separated two dielectrics in the transformed plane (in the target rectangle). When obtaining this curve, the capacitance of the system is calculated numerically by a finite-difference method.

We will employ the procedure developed in [10–12] to find air-dielectric boundary in the parallel-plate capacitors (step 5) with the difference that its capacitance will be calculated by Zehentner's technique [9].

Consider the sequence of the calculation in more detail. The composite forward mappings (1) from the original polygons z_{e1} and z_{o1} into target rectangles z_{e4} and z_{o4} (see Fig. 3 and Fig. 4) allow determining those dielectric-dielectric interface curves in the rectangles for the even (Fig. 6*a*) and odd (Fig. 6*b*) modes. It should be noted that the rectangle for the even mode has a magnetic slit, and therefore it can be more accurately described as a heptagon.

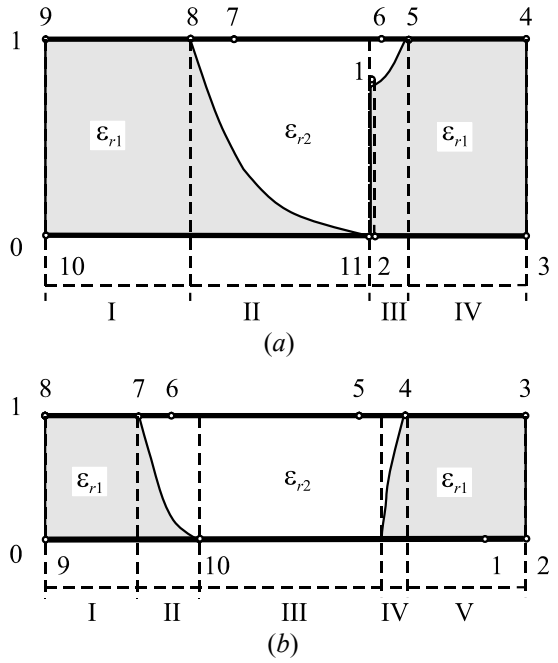

Fig. 6. Target rectangular regions of the half-structures (parallel-plate capacitors) of the coupled microstrip lines for the even (*a*) and odd (*b*) modes.

The rectangular regions with the electrodes placed on the upper and lower boundaries are divided by vertical magnetic walls into parallel subregions: four for the even mode (Fig. 6*a*) and five for the odd mode (Fig. 6*b*) respectively.

The first and fourth subregions for the even mode as well as the first, third and fifth subregions for the odd mode are filled with homogeneous dielectric. This allows immediate calculating the per-unit-length capacitance as the ratio of the width of the electrodes to the distance between them multiplied by the appropriate dielectric permittivity (Fig. 6).

The remaining second and third subregions for the even mode as well as the second and fourth subregions for the odd mode have inhomogeneous dielectric filling. The presence of the dielectric inhomogeneity requires further decomposition of the microstrip structure by the vertical magnetic walls (Fig. 6). The resulting narrow columnar subregions can be presented as a rectangular parallel-plate capacitor with an inclined interface line between dielectrics (Fig. 7).

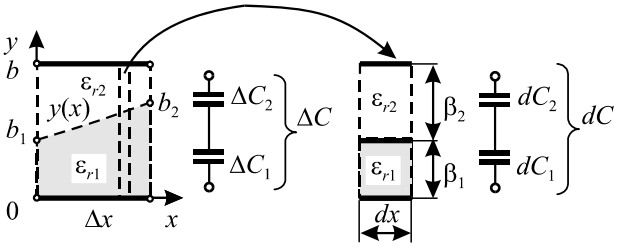

Fig. 7. The rectangular parallel-plate capacitor $\Delta x - b$ with inclined interface line $y(x)$ between dielectrics ε_{r1} and ε_{r2}.

In the rectangular parallel-plate capacitor $\Delta x - b$ with inclined interface line $y(x)$ between dielectric layers, the force lines of the electric field radiating from the upper conductor within the range Δx will almost perpendicularly intersect the curve $y(x)$ representing the surface of the dielectric in the microstrip structure [9]. The capacitance corresponding to this field can be simply determined as the capacitance of two sequentially connected capacitors.

Let Δx and b values denote respectively the width and outer spacing of their electrodes. Dielectric permittivities of the first and second capacitors are ε_{r1} and ε_{r2}, so that $\Delta\varepsilon = \varepsilon_{r2} - \varepsilon_{r1}$. In both capacitors, the spacing between their electrodes varies in the x direction, thus forming an inclined interface line $y(x)$ between dielectric layers. Assuming that the value x can be considered approximately as a constant within dx for chosen range Δx, the slope of the line $y(x)$ can be specified by following equation:

$$y(x) = ax + b_1, \tag{10}$$

where $a = (b_2 - b_1)/\Delta x$. Taking into account equalities $\beta_1 = y(x)$ and $\beta_2 = b - y(x)$, the capacitance dC of elementary parallel-plate capacitor with constant interface line can be expressed as:

$$dC = \left[dC_1^{-1} + dC_2^{-1} \right]^{-1} = \varepsilon_0 \left[\left(\frac{\varepsilon_{r1} dx}{\beta_1} \right)^{-1} + \left(\frac{\varepsilon_{r2} dx}{\beta_2} \right)^{-1} \right]^{-1}.$$

The total capacitance ΔC of the rectangular parallel-plate capacitor with the inclined interface line $y(x)$ between dielectrics with permittivities ε_{r1} and ε_{r2} is determined by following relation:

$$\Delta C = \int_0^{\Delta x} dC = \int_0^{\Delta x} \varepsilon_0 \left[\left(\frac{\varepsilon_{r1}}{\beta_1} \right)^{-1} + \left(\frac{\varepsilon_{r2}}{\beta_2} \right)^{-1} \right]^{-1} dx =$$

$$= \int_0^{\Delta x} \varepsilon_0 \left[\left(\frac{\varepsilon_{r1}}{y(x)} \right)^{-1} + \left(\frac{\varepsilon_{r2}}{b - y(x)} \right)^{-1} \right]^{-1} dx . \qquad (11)$$

The transformation of the formula (11) gives

$$\Delta C = \varepsilon_0 \int_0^{\Delta x} \left[\frac{ax + b_1}{\varepsilon_{r1}} + \frac{b - ax - b_1}{\varepsilon_{r2}} \right]^{-1} dx =$$

$$= \varepsilon_0 \int_0^{\Delta x} \frac{\varepsilon_{r1}\varepsilon_{r2} dx}{\frac{b_2 - b_1}{\Delta x}(\varepsilon_{r2} - \varepsilon_{r1})x + \varepsilon_{r2} b_1 + \varepsilon_{r1}(b - b_1)} . \qquad (12)$$

To transform (12), we apply the following known relation

$$\int \frac{dx}{Ax + B} = \frac{1}{A} \log \left| Ax + B \right| ,$$

As a result, we obtain

$$\Delta C = \frac{\varepsilon_0 \varepsilon_{r1} \varepsilon_{r2} \Delta x}{(\varepsilon_{r2} - \varepsilon_{r1})(b_2 - b_1)} \log \left[1 + \frac{(\varepsilon_{r2} - \varepsilon_{r1})(b_2 - b_1)}{\varepsilon_{r2} b_1 + \varepsilon_{r1}(b - b_1)} \right] .$$

This formula can be rewritten in the following alternative final forms:

$$\Delta C = \frac{\varepsilon_0 \varepsilon_{r1} \varepsilon_{r2} \Delta x}{(\varepsilon_{r2} - \varepsilon_{r1})(b_2 - b_1)} \log \left[\frac{\varepsilon_{r2} b_2 + \varepsilon_{r1}(b - b_2)}{\varepsilon_{r2} b_1 + \varepsilon_{r1}(b - b_1)} \right] =$$

$$= \frac{\varepsilon_{r1} \varepsilon_{r2} \Delta x}{(\varepsilon_{r2} - \varepsilon_{r1})(b_2 - b_1)} \log \left[\frac{(\varepsilon_{r2} - \varepsilon_{r1}) b_2 + \varepsilon_{r1} b}{(\varepsilon_{r2} - \varepsilon_{r1}) b_1 + \varepsilon_{r1} b} \right] . \qquad (13)$$

Expressions (13) specify the capacitance of rectangular parallel-plate capacitors with the inclined interface line $y(x)$ between dielectrics. These relations can be used to calculate per-unit-length capacitances of rectangular parallel-plate capacitors with real dielectric filling C_e, C_o for the even and odd modes.

Based on designations of Fig. 6, we have found even- and odd- mode capacitances with air $C_e(1)$, $C_o(1)$ and real dielectric filling C_e, C_o. They allow forming the per-unit-length matrices of the inductance L and the capacitance $C(1)$

$$L = \mu_0 \varepsilon_0 C(1)^{-1} ;$$

$$C(1) = \frac{1}{2} \begin{bmatrix} C(1)_o + C(1)_e & -C(1)_o + C(1)_e \\ -C(1)_o + C(1)_e & C(1)_o + C(1)_e \end{bmatrix} ,$$

where $\mu_0 = 400\pi$ nH/m. Capacitance matrix C per unit length in the case of real dielectric filling can be written as follows:

$$C = \frac{1}{2} \begin{bmatrix} C_o + C_e & -C_o + C_e \\ -C_o + C_e & C_o + C_e \end{bmatrix} .$$

At last, even- and odd- mode characteristic impedances and effective dielectric permittivities can be calculated by following well-known equations:

$$Z_{0(e,o)} = \frac{376.73}{\sqrt{\varepsilon_{eff(e,o)}} \left[C_{(e,o)}(1)/\varepsilon_0 \right]} ; \; \varepsilon_{eff(e,o)} = \frac{C_{(e,o)}}{C_{(e,o)}(1)} .$$

Furthermore, the average characteristic impedance and the coupling factor can be computed as

$$Z_0 = \sqrt{Z_{0e} Z_{0o}} ; \; k = (Z_{0e} - Z_{0o}) / (Z_{0e} + Z_{0o}) .$$

Results of simulation

As the test structure we choose coupled microstrip lines shown in Fig. 1 with the following physical and geometrical parameters: $w = 0.9$ mm; $t = 0.05$ mm; $s = 0.8$ mm; $h = 1$ mm; $\varepsilon_{r1} = 10$; $\varepsilon_{r2} = 1$.

Calculation of electric parameters by the proposed technique gives the following results: even/odd mode permittivities are $\varepsilon_{effe} / \varepsilon_{effo} = 6.45 / 5.25$, characteristic impedances are $Z_{0e} / Z_{0o} = 61.3 / 42.2$ Ohms; $Z_0 = 51$ Ohm; $k = 15$ dB.

The same parameters obtained by the program LINPAR (method of moments) [19] are as follows: $\varepsilon_{effe} / \varepsilon_{effo} = 7.06 / 5.41$; $Z_{0e} / Z_{0o} = 60.0 / 41.8$ Ohms; $Z_0 = 50$ Ohm; $k = 15$ dB.

The same parameters obtained by the program AWR/TXLINE: $\varepsilon_{effe} / \varepsilon_{effo} = 7.21 / 5.85$; $Z_{0e} / Z_{0o} = 57.2 / 41.4$ Ohms; $Z_0 = 49$ Ohm; $k = 16$ dB.

One can see that the difference between numerical results for the characteristic impedance and even/odd mode permittivities does not exceed 1—4% and 3—10% respectively. It should be noted that the proposed technique allows analyzing the more complex structures with vertical substrates [3] which can not be calculated by the planar modeling system AWR/TXLINE.

Conclusion

The effective technique based on free computer package of the Schwarz–Christoffel toolbox for MATLAB implemented the numerical conformal

transformation has been proposed. This technique allows calculating the microstrip structures with complicated cross-section. The electric field distribution in the analyzed structure and line shapes between dielectrics in the target rectangular region (parallel-plate capacitor) can be successfully determined by proposed technique.

To verify the developed approach, the coupled microstrip lines have been modeled with taking into account the conductor thickness. The simulated results are in good agreement with the calculated data obtained by other well-known computer programs. The described approach is characterized by high numerical efficiency and accuracy appropriate for practical applications.

Acknowledgment

The authors are indebted to M. Goano, Politecnico di Torino, Turin, Italy, and to T. Driscoll, University of Delaware, Newark, DE, USA for helpful advice and discussion.

This work was partially supported by Ministry of Education and Science of Russia, Federal Targeted Programm "Scientific and Scientific-Pedagogical Personnel of the Innovative Russia" for 2009─2013, Research Works in the Direction "Microelektronics".

References

1. Field modeling of a multiconductor digital bus / H. Yordanov, M. Ivrlac, J. Nossek, P. Russer // Proceedings of the 37th European Microwave Conference, October 8─12, 2007. ─ Munich, Germany, 2007. ─ P. 1377─1380.

2. Sychev A. N., Chekalin M. E. Numerical conformal transformations technique for analysis of the microstrip structures // Proceedings of 21st International Crimean Conference "Microwave & Telecommunication Technology", September 12─16, 2011. ─ Sevastopol: Weber, 2011. ─ P. 216─218.

3. Sychev A. N., Dolgushin M. E. Analysis of the broadside coupled lines on the vertical substrate using the numerical conformal transformations // Proceedings of 20th International Crimean Conference "Microwave & Telecommunication Technology", September 13─17, 2010. ─ Sevastopol: Weber, 2010. ─ P. 636─638.

4. Ghione G., Goano M. Revisiting the partial-capacitance approach to the analysis of coplanar transmission lines on multilayered substrates // IEEE Transactions on Microwave Theory and Techniques. ─ 2003. ─ Vol. 51, N. 9. ─ P. 2007─2014.

5. A general conformal-mapping approach to the optimum electrode design of coplanar waveguides with arbitrary cross section / M. Goano, F. Bertazzi, P. Caravelli, G. Ghione, T. Driscoll // IEEE Transactions on Microwave Theory and Techniques. ─ 2001. ─ Vol. 49, N. 9. ─ P. 1573─1580.

6. Teppati V., Goano M., Ferrero A. Conformal-mapping design tools for coaxial coupler with complex cross section // IEEE Transactions on Microwave Theory and Techniques. ─ 2002. ─ Vol. 50, N. 10. ─ P. 2339─2345.

7. Sychev A. N. A simple technique of enclosed subregions for CAD models of shielded multilayer/multiconductor coplanar coupled lines // Proceedings of Asia-Pacific Microwave Conference, December 2002 ─ Kyoto, Japan, 2002. ─ Vol. 1. ─ P. 85─88.

8. Sychev A. N. Combined method of partial capacitances and conformal mapping for analysis of multimode stripline structures. ─ Tomsk: TUSUR Publisher, 2007. ─ 138 p. [in Russian].

9. Zehentner J. Characteristic impedance and effective permittivity of modified microstrip line for high power transmission // IEEE Transactions on Microwave Theory and Techniques. ─ 1987. ─ Vol. 35, N. 7. ─ P. 615─620.

10. Wheeler H. A. Transmission line properties of parallel strip separated by dielectric sheet // IEEE Transactions on Microwave Theory and Techniques. ─ 1965. ─ Vol. 13, N. 3. ─ P. 172─185.

11. Wan C. Analytically and accurately determinated quasi-static parameters of coupled microstrip lines // IEEE Transactions on Microwave Theory and Techniques. ─ 1996. ─ Vol. 44, N. 1. ─ P. 75─80.

12. Callarotti R., Gallo A. On the solution of a microstripline with two dielectrics // IEEE Transactions on Microwave Theory and Techniques. ─ 1984. ─ Vol. 32, N. 4. ─ P. 333─339.

13. Lavrik V. I., Fil'chakova V. P., Yashin A. A. Conformal mapping of physic-topological models / Ed. by Yu. A. Mitropol'sky. ─ Kiev: Naukova Dumka, 1990. ─ 376 p. [in Russian].

14. Driscoll T. SC toolbox for MATLAB. http://www.math.udel.edu/~driscoll/SC.

15. Driscoll T. A. Algorithm 756: A MATLAB toolbox for Schwarz–Christoffel mapping // AMC Transactions on Mathematical Software. ─ June 1996. ─ Vol. 22, N. 2. ─ P. 168─186.

16. Driscoll T. A. Algorithm 843: Improvements to the Schwarz–Christoffel Toolbox for MATLAB // ACM Transactions on Mathematical Software. ─ June 2005. ─ Vol. 31, N. 2. ─ P. 239─251.

17. Crowdy D. G. The Schwarz–Christoffel mapping to bounded multiply connected polygonal domains // Proceedings of the Royal Society, A 461. ─ 2005. ─ P. 2653─2678.

18. Crowdy D. G. The Schottky–Klein prime function on the Schottky double of planar domains // Computational Methods and Function Theory. ─ 2010. ─ Vol. 10, N. 2. ─ P. 501─517.

19. LINPAR for Windows: Matrix parameters for multiconductor transmission lines / A. Djiordjevic, M. B. Bazdar, T. K. Sarkar, R. F. Harrington // Software and user's manual. ─ 1995.

Received in final form January 29, 2012